

## **HYDRATED PHASES IN BLENDED CEMENTITIOUS SYSTEMS FOR NUCLEAR INFRASTRUCTURE**

**Kenneth A. Snyder (1), Paul E. Stutzman (1), Jacob Philip (2) and David Esh (2)**

(1) National Institute of Standards and Technology,  
100 Bureau Drive  
Gaithersburg, MD 20899-8615  
USA

(2) U.S. Nuclear Regulatory Commission, Washington, DC USA

Keywords: cement hydration; materials characterization; quantitative X-ray diffraction; Rietveld analysis; thermodynamic hydration modeling; thermogravimetric analysis;

# HYDRATED PHASES IN BLENDED CEMENTITIOUS SYSTEMS FOR NUCLEAR INFRASTRUCTURE

**Kenneth A. Snyder (1), Paul E. Stutzman (1), Jacob Philip (2) and David Esh (2)**

(1) National Institute of Standards and Technology, Gaithersburg, MD USA

(2) U.S. Nuclear Regulatory Commission, Washington, DC USA

## **Abstract**

The hydration products of varying proportions of portland cement, fly ash, ground granulated blast furnace slag, and silica fume in blended systems were identified and quantified. The proportion of portland cement varied from 100 % to 10 %. Each binder was characterized by its oxide content, and all the pastes were made at constant water:cementitious material mass ratio. The hydrated paste samples were analyzed using a combination of Rietveld analysis of X-ray diffraction data and thermogravimetric analysis. The estimated type and quantity of phases present were compared to current thermodynamic models for blended cement hydration. Results are given after three months hydration, and the research program is part of a year-long study that will include X-ray microanalysis and pore solution analysis. The techniques and data from this experiment will be used to evaluate hydrated systems and to validate the hydrated phase prediction component of performance assessment computer models for nuclear applications.

## **1. INTRODUCTION**

The various infrastructure elements of future nuclear facilities may be composed of the broad range of cementitious binder proportions: structural elements may be composed entirely of portland cement concrete; massive concrete elements may contain large quantities of fly ash and/or ground granulated blast furnace slag (GGBFS); and saltstone grouts<sup>1</sup> may contain less than 10 percent portland cement, with fly ash and slag making up the remainder. Improved performance assessment (PA) tools are needed for predicting the performance of all these systems because existing tools were developed for systems composed mostly of portland cement. An important component of these tools is the ability to estimate the type and quantity of hydrated phases present, and the pore solution composition, as these factors impact overall performance because they control, among other things, the buffering capacity of the material, the mobility of certain radionuclides, and the chemical composition of the effluent.

Sophisticated computer tools for predicting transport and reaction in cementitious systems incorporate thermodynamic data for the mineral phases present. Transport of ions from the

external ground water changes the chemical equilibrium, and the thermodynamic model adjusts the quantity of phases to maintain equilibrium. Therefore, an accurate assessment/prediction of the initial hydrated phases and pore solution composition is vital component to an accurate PA tool.

To validate the hydrated phases prediction component of PA tools, standardized materials characterization techniques are needed to identify the phases in existing materials. In addition, system characterization data are required for model validation. Two very useful characterization tools are X-ray powder diffraction (XRD) and thermogravimetric analysis (TGA). XRD measures angular-dependent reflection from crystalline phases, and Rietveld analysis of the XRD data yields the phase mass ratios. When amorphous material is present, a known amount of a unique crystalline material is added to the sample, and then Rietveld analysis can be used to determine the quantity of all the crystalline phases present, and the amorphous fraction by difference. TGA consists of monitoring sample mass loss during heating in an inert atmosphere. Many of the phases present in hydrated cement paste contain chemically bound water, and these hydrated phases release the bound water at specific temperatures. If the temperature range over which the mass loss occurs can be identified and is isolated from the mass loss from other phases, one can use TGA to identify and quantify phases that are present.

X-ray diffraction characterization techniques for quantifying hydrated cementitious phases differ from that for quantifying portland cement. Portland cement contains virtually no amorphous material, obviating the need for an internal crystalline standard. Also, cement XRD characterization techniques have been standardized and documented.<sup>2</sup> Hydrated cementitious systems, by contrast, contain a majority mass fraction of amorphous material. The approach of adding an inert crystalline material at the time of mixing may have an undesirable effect on the rate of hydration. Alternatively, adding a known amount of an internal standard to a sample of hydrated paste requires moisture stabilization to reach equilibrium with the laboratory atmosphere, and this can affect the structure of those phases that are sensitive to changes in temperature and humidity (e.g., ettringite, monosulfate, etc.).

As an alternative to adding an internal standard, TGA is used to quantify the calcium hydroxide (portlandite) present in the system. The water loss during conversion of portlandite to calcium oxide (lime) happens at a distinct and identifiable temperature. Because other hydrated phases are losing water over the same temperature range (but at a much slower rate), the analysis of the portlandite peak must account for the background mass loss.

The type and quantity of hydrated phases in paste samples are estimated by combining XRD and TGA data for blended systems having portland cement mass fractions varying from 100 % to 10 %. The XRD data are used to identify the mineral phases present, and the relative mass fractions of each phase. TGA is used to estimate the portlandite content, from which the absolute mass fraction of each phase is estimated. The results are compared to estimates from a thermodynamic hydration model.

2.

**EXPERIMENTAL PROGRAM**

Eight cement paste mixtures were developed to span the range of cementitious binder mixtures anticipated for nuclear applications. The mass fractions of cement, fly ash, ground granulated blast furnace slag (GGBFS), and silica fume for each of the eight mixtures are given in Table 1.

**Table 1:** Mixture mass fractions of the cementitious binders in each mixture.

Mix #	Cement	Fly Ash	GGBFS	Silica Fume
1	1.00			
2	0.70	0.30		
3	0.70		0.30	
4	0.70	0.20		0.10
5	0.50	0.50		
6	0.50		0.50	
7	0.30	0.35	0.35	
8	0.10	0.45	0.45	

All the materials are commercial products. The ASTM Type I/II portland cement contained 3.5 % limestone by mass and had a Blaine fineness of 372 m<sup>2</sup>/kg. The fly ash is an ASTM Type C, and the GGBFS and the silica fume were commercial products. The oxide mass fractions were measured by a commercial laboratory, and the values are given in Table 2. The slag contained no crystalline phases, and the fly ash contained 7 % quartz, 5 % mullite, and 2 % hematite by mass. Also given in the table are the cement calcite content and the slag sulfide content.

**Table 2:** Oxide mass fractions for the binders. The cement calcite content and the slag sulfide content are also given.

Phase	Cement	Fly Ash	GGBFS	Silica Fume
CaO	0.605	0.246	0.371	0.005
SiO <sub>2</sub>	0.191	0.370	0.373	0.962
Al <sub>2</sub> O <sub>3</sub>	0.050	0.200	0.104	0.003
Fe <sub>2</sub> O <sub>3</sub>	0.033	0.053	0.005	0.000
MgO	0.041	0.048	0.116	0.001
SO <sub>3</sub>	0.031	0.014	0.022	0.000
Na <sub>2</sub> O	0.001	0.015	0.002	0.001
K <sub>2</sub> O	0.007	0.006	0.003	0.005
TiO <sub>2</sub>	0.003	0.016	0.005	0.000
CaCO <sub>3</sub>	0.034			
Sulfide			0.010	

The paste specimens were made by combining the dry binder, adding distilled water, mixing in a blender, and then casting into 25 mm diameter, 25 mm tall cylinders. The cylinders were placed into re-sealable bags and kept in a walk-in environmental chamber maintained at 25 °C. The samples were demolded after 24 hours (48 hours for Mix 7 and Mix 8), and placed into a sealed jar that was stored in the walk-in environmental chamber. At  $(12 \pm 1)$  weeks of hydration, individual samples approximately 1 mm thick were cut from the specimen on a diamond saw using ethanol as the cutting lubricant; the first 1 mm at the surface was discarded. After cutting each sample, the surface was cleaned with a soft plastic-bristled brush and rinsed with ethanol.

The XRD sample was used as is, without being ground to a powder. Before mounting into the XRD sample holder, the paste sample was polished briefly using 600 grit emery abrasive paper and ethanol, and then cleaned again with the brush and rinsed with ethanol. During the XRD measurement, the sample was rotated to reduce the effects of preferred orientation by increasing the sampling volume.

The TGA sample (typically 50 mg) was a 1 mm slice cut from the original cylindrical specimen, ground to a powder using a mortar and pestle, and then analyzed using a commercial TGA in which the sample chamber was purged with high purity nitrogen. The TGA procedure for each sample was to first bring the sample to equilibrium at 30 °C, and then record the mass as the temperature increased to 950 °C at a heating rate of 5 °C/min.

### 3. RESULTS

The TGA data were first re-scaled using the initial mass. The device records the sample mass  $m$  as a function of the temperature  $T$ . The scaled mass  $\mu$  is the recorded mass divided by the initial mass  $m_0$ : ( $\mu = m/m_0$ ). The differential scaled mass loss ( $-d\mu/dT$ ) for each of the eight mixes after 12 weeks of hydration is given in Figure 1.

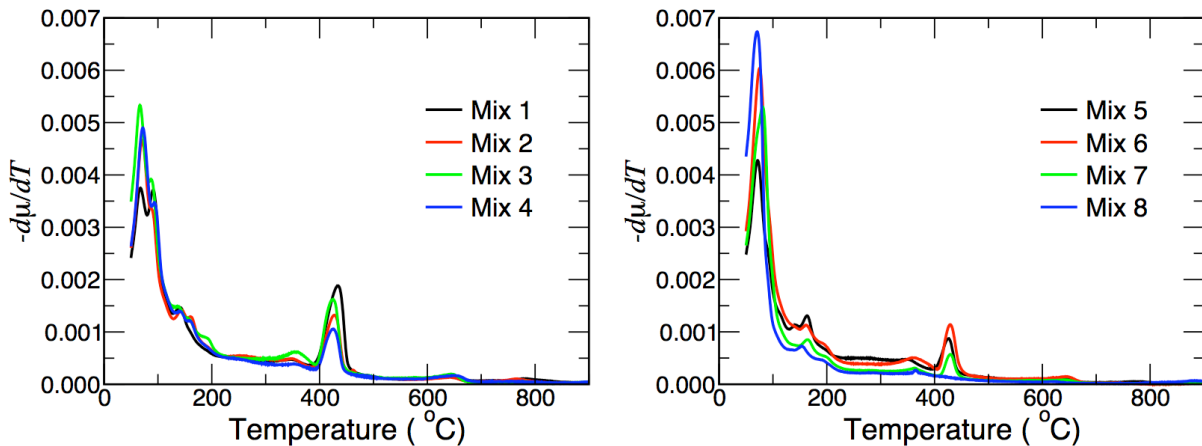


**Figure 1:** Thermogravimetric data for Mix 1-4 (l) and Mix 5-8 (r) after 12 weeks of hydration.

The peak at approximately 425 °C, is due to loss of water in the conversion of portlandite to lime. The portlandite peak prominence and separation is exploited to obtain an estimate for the portlandite content. This value is then used to establish the quantity of portlandite for the XRD Rietveld analysis. The portlandite mass fractions for the mixtures in Figure 1 are reported in Table 3.

**Table 3:** Estimated portlandite mass fraction as calculated from TGA data. The parameter coefficient of variation reported by the regression software was typically less than 0.3 %, and other comparisons to XRD data were generally within 2 %.

Mix	Portlandite Mass Fraction	Mix	Portlandite Mass Fraction
1	0.119	5	0.031
2	0.064	6	0.039
3	0.063	7	0.019
4	0.049	8	-

No portlandite was detected in Mix 8. Therefore, corundum (87 % crystalline) was added as an internal standard. To stabilize the powder mass prior to adding the corundum, the sample was dried briefly in a 60 °C oven. Prior to adding the corundum, a small portion was taken and analyzed by TGA to estimate the adjusted water content so that the corundum mass fraction could be expressed as a mass fraction of the original sample.

The XRD data for the 12 week samples were obtained from a commercial XRD apparatus designed for powder specimens and having a Cu-K $\alpha$  X-ray source. Data were obtained with  $2\theta$  step size of 0.016°, and sampled for more than 1 s per step. The XRD data from all 8 mixes are shown in Figure 2, with individual scans offset from one another for comparison purposes. Sequential repetitions on a single sample showed no measurable difference in the XRD data.

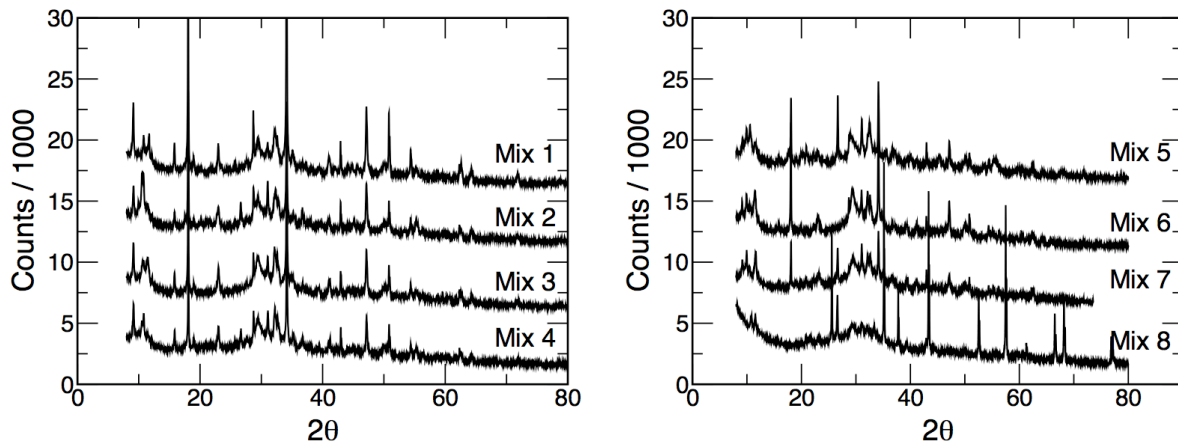


**Figure 2:** XRD scans for all 8 mixes. The upper curves are displaced from the immediately lower curve by a value of 5.

Rietveld analysis was performed using the data from the range  $8^\circ \leq 2\theta \leq 80^\circ$ . The structural models for the cement phases were taken from Stutzman and Leigh.<sup>2</sup> The available structural models for the hydrated phases were obtained from public web sites.<sup>3</sup> The structural model for hemicarbonates was created using structural information from Taylor.<sup>4</sup> The amorphous ‘hump’ in the range  $20^\circ \leq 2\theta \leq 40^\circ$  was approximated by amorphous silica using the approach of Le Bail.<sup>5</sup> Quartz was the only crystalline phase from the fly ash that remained after 12 weeks of hydration. The final results of the Rietveld analysis are given in

Table 4, and the refinement estimated standard deviation for each crystalline phase was rarely greater than 0.002.

Mix 8 required special consideration. The XRD data range was expanded to  $6^\circ \leq 2\theta \leq 80^\circ$  to quantify the strätlingite. To accommodate changes in Mix 8 that occurred while drying to prepare for the corundum addition, the amounts of C<sub>2</sub>S and periclase were assumed to remain unchanged, allowing the Rietveld analysis results to be expressed as a mass fraction of the original material.

Furthermore, the nearly equal mass fractions of unhydrated C<sub>3</sub>S in both Mix 1 and Mix 8 suggests that the uncertainty in the determination of low mass fraction phases may be greater than the 10 % relative error reported by the Rietveld software. Therefore, phases with mass fractions below approximately 2 % may be better categorized as ‘trace’.

**Table 4:** Hydrated phase mass fractions after 3 months hydration at 25 °C, as determined by Rietveld analysis. Mix 1 through Mix 7 use the portlandite content (see Table 3) as the internal standard. Mix 8 uses corundum as an internal standard.

	Mix 1	Mix 2	Mix 3	Mix 4	Mix 5	Mix 6	Mix 7	Mix 8
Amorphous	0.600	0.691	0.674	0.749	0.730	0.785	0.751	0.816
C <sub>3</sub> S	0.013	0.014	0.041	0.023	0.033	0.021	0.017	0.014
β-C <sub>2</sub> S	0.060	0.037	0.037	0.027	0.040	0.014	0.028	0.016
C <sub>3</sub> A	0.002	0.001			0.003		0.001	0.008
C <sub>4</sub> AF	0.027	0.017	0.019	0.011	0.009	0.006	0.013	0.013
Portlandite	0.119	0.064	0.063	0.049	0.031	0.039	0.019	
Ettringite	0.075	0.041	0.052	0.052	0.015	0.019	0.034	0.016
Calcite	0.014	0.014	0.018	0.019	0.011	0.024	0.016	0.013
Monocarbonate	0.058	0.042	0.040	0.028	0.051	0.030	0.038	0.028
Periclase	0.012	0.009	0.008	0.007	0.006	0.003	0.006	0.006
Hemicarbonate	0.015	0.032	0.015	0.016	0.016	0.008	0.006	0.007
Quartz		0.015	0.003	0.010	0.025	0.002	0.017	0.026
Monosulfate	0.007	0.018	0.008	0.011	0.029	0.018	0.028	0.018
Hydrotalcite		0.004	0.024			0.032	0.026	0.019
Strätlingite								0.009

## 4.

## THERMODYNAMIC CALCULATIONS

The thermodynamic hydration model of Lothenbach et al.<sup>6</sup> was used to estimate the type and quantity of phases present after 3 months hydration. The model has equations characterizing the rate of portland cement hydration. By contrast, there are no established rate equations for fly ash, slag, and silica fume hydration, and a complementary experimental program would be required to identify the relevant material properties for establishing a model. For this calculation, the maximum fraction of each supplemental material that was allowed to hydrate was adjusted to approximate the measured quantities. Results from the calculations are given in Table 5.

There is general agreement between the observed and the predicted phases present. The thermodynamic model assumed a greater degree of reactivity for the periclase and the calcite, and the quantity of quartz could have been approximated by assuming zero reactivity. As expected, the quantity of each phase differs, but this is due, in large part, to uncertainty in estimating the degree of reactivity for each of the supplementary materials.

**Table 5:** Estimated phase mass fractions after 3 months hydration as calculated using the Lothenbach et al.<sup>6</sup> thermodynamic hydration model.

	Mix 1	Mix 2	Mix 3	Mix 4	Mix 5	Mix 6	Mix 7	Mix 8
Amorphous	0.362	0.544	0.531	0.605	0.673	0.652	0.796	0.886
C <sub>3</sub> S	0.026	0.016	0.016	0.016	0.012	0.012	0.007	0.002
$\beta$ -C <sub>2</sub> S	0.069	0.049	0.049	0.049	0.035	0.035	0.021	0.007
C <sub>3</sub> A	0.002	0.001	0.001	0.001	0.001	0.001	0.001	0.000
C <sub>4</sub> AF	0.017	0.011	0.011	0.011	0.008	0.008	0.005	0.002
Portlandite	0.127	0.054	0.064	0.013	0.030	0.027	0.006	
Ettringite	0.144	0.080	0.109	0.100	0.041	0.079	0.045	0.017
Calcite	0.008		0.003	0.002				
Monocarbonate	0.102	0.101	0.085	0.092	0.072	0.072	0.015	0.014
Periclase								
Hemicarbonate							0.056	
Quartz								
Monosulfate		0.036			0.051	0.008		
Hydrotalcite				0.020	0.009	0.039	0.006	0.002
Strätlingite								0.037



## **5. DISCUSSION**

The methods used here for characterizing hydrated phases will require further development and refinement. Using amorphous silica to approximate the amorphous phases is useful in representing the XRD data background, but further work is needed to validate the approach. Later in this project, using TGA to estimate portlandite content will have limited applicability as a number of these mixes will eventually consume the portlandite. Predictive hydration models will require new characterization techniques and data before they can accurately predict the rate of reaction for fly ash and slag in blended systems.

Later in this project, additional experimentation will be conducted to independently verify results to date. X-ray microanalysis will be used to develop chemical maps of the microstructure. Using these maps, the relative proportions of elements, along with visual observation, will be used to classify distinct mineral phases. This information can then be used to segment the entire image into their constituent phases. These data can then be used to validate the XRD data.

Additionally, the pore solution can be extracted and analyzed to determine the concentration of elements present. This information would have two uses. First, the data could be used to validate models that predict pore solution composition. The challenge for these models is to predict the oxidation state and the alkali (sodium and potassium) concentrations. The oxidation state is vital to predicting the mobility of radionuclides such as technetium, and the alkali concentration can vary due to alkalis incorporated into the C-S-H.<sup>7</sup> Second, a thermodynamic model can be used to confirm whether phases are saturated with respect to the pore solution composition.

Ultimately, these data and the techniques will support the development of new tools for future performance assessments (PA). These tools will need to accurately predict the mineralogy and pore solution composition for a wide range of cementitious systems. The data and techniques developed in this project will ultimately be used to validate the hydration component of these models.

## **6. CONCLUSION**

Combining thermogravimetric data with X-ray diffraction data shows promise for characterizing the type and quantity of hydrated phases in blended cement systems. The phases identified are consistent with current thermodynamic models, but further research is needed to quantify the rate of reaction of fly ash and slag. Further experimentation is needed, however, to independently validate the quantity of phases observed through XRD and TGA.

## **ACKNOWLEDGEMENTS**

The authors also wish to thank Dr. Barbara Lothenbach (EMPA) for her assistance with the thermodynamic calculations.

## **REFERENCES**

- 
- <sup>1</sup> Bradford, A., Esh, D., Ridge, A, Thaggard, M., Whited, R., Treby, S., Flanders, S. and Camper, L.W., 'U.S. Nuclear Regulatory Commission Technical Evaluation Report for the U.S. Department of Energy Savannah River Site Draft Section 3116 Waste Determination for Salt Waste Disposal,' Technical Report (U.S. Nuclear Regulatory Commission, Washington, D.C., 2005).
- <sup>2</sup> Stutzman, P. and Leigh, S., 'Phase Composition Analysis of the NIST Reference Clinkers by Optical Microscopy and X-ray Powder Diffraction,' NIST Technical Note 1441 (National Institute of Standards and Technology, Gaithersburg, MD, 2002)
- <sup>3</sup> <http://rruff.geo.arizona.edu/AMS/amcsd.php> & <http://database.iem.ac.ru/mincryst/>
- <sup>4</sup> Taylor, H.F.W., 'Cement Chemistry', (Academic Press, New York, 1990).
- <sup>5</sup> Le Bail, A., 'Modelling the silica glass structure by the Rietveld method,' *J. Non-Cryst. Solids* **183** (1995) 39-42.
- <sup>6</sup> Lothenbach, B., Le Saout G., Gallucci, E., Scrivener, K., 'Influence of limestone on the hydration of Portland cements,' *Cem. Concr. Res.* **38** (2008) 848-860.
- <sup>7</sup> Taylor, H.F.W., 'A method for predicting alkali ion concentrations in cement pore solutions,' *Adv. Cem. Res.* **1** (1987) 5-17.